Characteristics of a large volume, helicon plasma source

Shunjiro Shinohara[a)]
Interdisciplinary Graduate School of Engineering Sciences, Kyushu University, Kasuga, Fukuoka 816-8580, Japan

Takao Tanikawa
Research Institute of Science and Technology, Tokai University, Hiratsuka, Kanagawa 259-1292, Japan

(Received 20 August 2004; accepted 15 December 2004; published online 16 March 2005)

A high-density helicon plasma source with very large volume, 75 cm in diameter and 486 cm in axial length, has been developed, and its characteristics have been investigated. Furthermore, the radial density profile control has been successfully demonstrated by utilizing two techniques: (1) by changing the magnetic field configurations near the antenna and (2) by changing the antenna radiation-field patterns. Using two types of large-diameter spiral antennae, plasma with density exceeding 10^{12} cm^{-3} has been produced with several hundreds of watts of radio frequency power. By changing the magnetic field configuration near the antenna, the threshold power and the degree of the density change in a density jump can be varied. The electron density reaches the maximum away from the antenna; then decays weakly along the axial direction. © *2005 American Institute of Physics*. [DOI: 10.1063/1.1861058]

Developing a large volume plasma source capable of producing a high density, current-free plasma is very important for many fields; profile control under various magnetic field configurations is also much needed. A helicon plasma source[1–10] that employs helicon waves for plasma production has been extensively investigated as a very efficient source of current-free dense plasma for both fundamental research and numerous application studies. However, most helicon sources are small, typically less than 10 cm in diameter, and radial density profile control has not been seriously attempted in spite of the fact that this control is a critical problem to be solved.

Large helicon sources have been developed at some institutions,[11–13] using spiral antennae installed at just outside the vacuum chamber. However, detailed plasma characterization and the radial profile control have not been sufficiently investigated. In this Brief Communication, we present in more detail the characteristics and the profile control of a very efficient, large-volume helicon plasma source[13] (75 cm in diameter and 486 cm in axial length) at the Institute of Space and Astronautical Science (ISAS), a division of the Japan Aerospace Exploration Agency (JAXA). The dependences of the electron density on various parameters have been carefully investigated, and innovative methods of controlling plasma profiles were demonstrated by changing the magnetic field configurations and by changing the antenna radiation-field patterns. The details of the experimental setup is described in Ref. 13.

First, we present the experimental results showing the highly efficient production of high-density plasma. Throughout the paper, unless denoted specifically, the full spiral turns with the high voltage (ground) feeding point being the outer side (center) of the antenna are used in a pulsed discharge mode. Figure 1 shows the relationships between the plasma densities n_e and the input rf power P_{inp}, changing the separate coil current I_s, which can change the strength of the magnetic field near the type *A* antenna (6 turns with 23 cm in outer diameter).[13] Plasma can be initiated at as low as $P_{inp} \sim 1$ W, where n_e is on the order of 10^9 cm^{-3}. The discharge mechanism in this low density regime may be categorized as a capacitively coupled plasma (CCP) discharge.[6] Wave propagation along the *z* axis is not observed before the density jump, and as is often seen[14] with increasing rf power, plasma behavior alters from CCP to helicon plasma discharge (HP) through inductively coupled plasma (ICP).[6,15] With the increase in P_{inp}, n_e increases. When P_{inp} exceeds the threshold power P_{th}, that is in a range of 70–300 W, a so-called "density jump" to the order of 10^{12} cm^{-3} is observed. It can be seen that both P_{th} and the large density increment of Δn_e increase as the separate coil current I_s is increased. Note that the densities just before and after the jump also increase with I_s. This behavior agrees with the results of earlier experiments[16] and numerical results,[17] using a loop antenna wound around a small glass tube, and also with recent numerical results[18] calculated for nearly the same conditions as the present experiments using a spiral antenna. The value of P_{th} tends to decrease with the increase in Ar fill pressure P_{Ar}.

We have verified, through the measurements of the wave dispersion relation, that the discharge mechanism after the jump is indeed based on helicon waves by monitoring the axial component of the rf magnetic field. The electron density as a function of the input rf power for the type *B* antenna[13] (4 turns with 43 cm in outer diameter) shows the same tendency as with the type *A* antenna. The maximum density obtained so far is 2.5×10^{12} cm^{-3} by the use of the type *B* antenna, with $P_{inp}=549$ W, $P_{Ar}=0.5$ mTorr, $I_m=286$ A (corresponding to a main field of 800 G), and $I_s=16$ A. This maximum density is only limited by the capability of our rf amplifier, less than 1 kW. An even higher

[a)]Electronic mail: sinohara@aees.kyushu-u.ac.jp

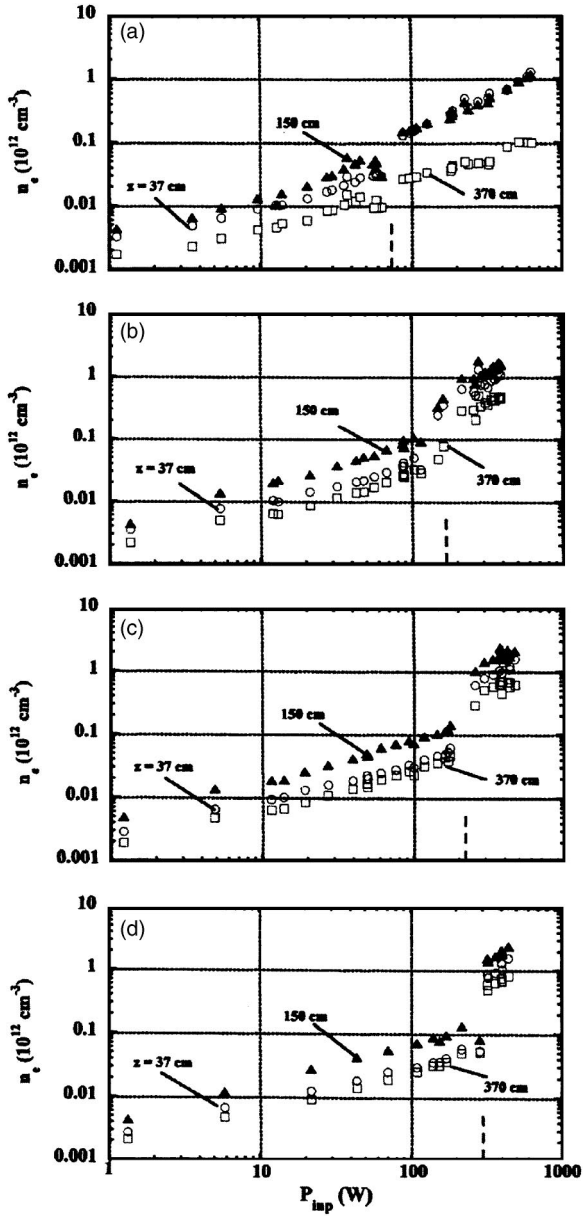

FIG. 1. Relationship between the electron density n_e and the input rf power P_{inp}, changing the separate coil current I_s near the type *A* antenna: I_s=(a) 0 A, (b) 5 A, (c) 10 A, and (d) 15 A. Here, fill pressure is P_{Ar}=2 mTorr and the main field is 140 G (main coil current I_m=50 A). Open circles, closed triangles, and open boxes show measurements at z=37 cm, 150 cm, and 370 cm, respectively. Vertical dotted lines denote the threshold rf input power P_{th} for the density jump.

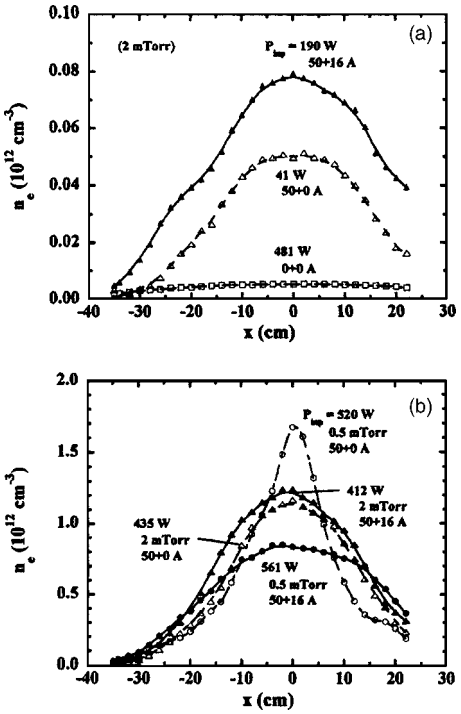

FIG. 2. Radial profiles of n_e at z=150 cm, changing the magnetic field configurations with the type *B* antenna: (a) Open boxes, open triangles, and closed triangles show (I_m,I_s)=(0 A,0 A), (50 A,0 A), and (50 A,16 A), respectively, with P_{Ar}=2 mTorr; and (b) open and closed circles (open and closed triangles) mean (I_m,I_s)=(50 A,0 A) and (50 A,16 A), respectively, with P_{Ar}=0.5(2) mTorr.

density should be able to be obtained with a more powerful rf amplifier.

Next, we present the results of the radial and axial plasma profiles under various conditions. First, control of the radial electron density profile has been attempted by changing the magnetic field configuration near the antenna, which can be achieved by varying I_s, as well as by changing the antenna radiation-field pattern in two ways. Figure 2 shows the radial profiles of the electron density measured at z =150 cm using the former method, i.e., the magnetic field effect, with the type *B* antenna. These profiles are taken before [Fig. 2(a)] and after [Fig. 2(b)] the density jumps, changing I_s with the constant main field of 140 G except for one case in Fig. 2(a), which has no magnetic field (I_m=I_s=0 A). As shown in Fig. 2(a), in which CCP/ICP discharges are expected, the magnetized plasma column with n_e on the order of 10^{10} cm^{-3} has a rather broad radial density profile, and this profile becomes broader with the increase in I_s from 0 to 16 A: the full width at half maximum (FWHM) widens from 35 to 42 cm. In the case of no magnetic field, i.e., I_m=I_s=0 A, the plasma is much more uniform along the radial direction (FWHM is ~60 cm), although the density is low ($<6\times10^9$ cm^{-3}) due to the monotonic decrease in n_e in the axial direction [see Fig. 6(a)]. After the density jump, the discharge mode changes to the HP mode; the plasma column also has a broader radial density profile with the increase in I_s. This tendency is much clearer especially for low P_{Ar}: FWHM is 16 (40) cm with I_m=50 A, I_s=0 (16) A, and P_{Ar} =0.5 mTorr, while FWHM is 30 (33) cm with I_m=50 A, I_s =0 (16) A, and P_{Ar}=2 mTorr.

The dependence of the radial profile on I_s after the jump can be understood as follows: the degree of field convergence from the antenna region to the main field region becomes weaker (that is, field uniformity improves near the antenna) as I_s is increased; as a result, the plasma flows (the plasma is also generated in the wave excitation region) more naturally along the field line to make the radial density profile broader. Considering the discussions of the magnetic field configurations, a much more peaked radial density profile can be realized with a larger main field strength. For example, FWHM is quite narrow (13 cm) with I_s=16 A and

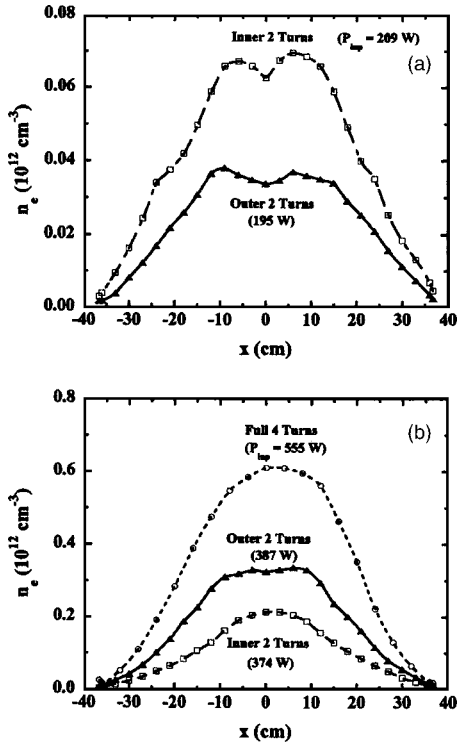

FIG. 3. Radial profiles of n_e at $z=150$ cm, changing electrical connections of taps in the type *B* antenna with $P_{Ar}=0.5$ mTorr, $I_m=50$ A, and $I_s=16$ A: (a) Closed triangles and open boxes show the cases having outer 2 turns and inner 2 turns, respectively, before the density jumps; and (b) open circles, closed triangles, and open boxes denote the cases of 4 full turns, outer 2 turns, and inner 2 turns, respectively, after the density jumps.

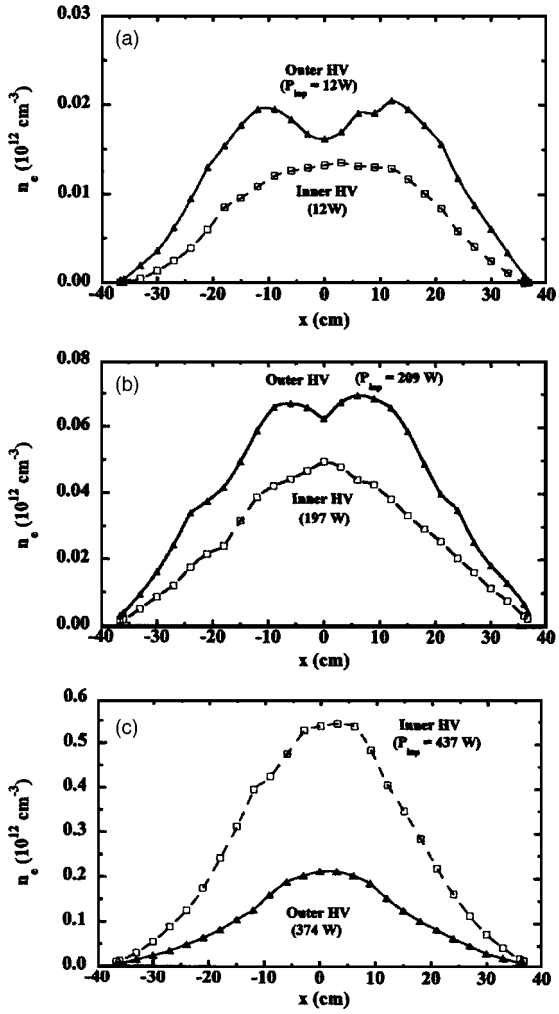

FIG. 4. Radial profiles of n_e at $z=150$ cm, changing the electrical connections of the taps in the type *B* antenna (using inner 2 turns) with $P_{Ar}=0.5$ mTorr, $I_m=50$ A, and $I_s=16$ A. Here, closed triangles (open boxes) denote the high voltage side of the rf input being at the outer side (inner side) of the antenna. Here, P_{inp} is increased from (a) to (c); cases (a) and (b) are taken before the density jumps, and case (c) is after the jumps.

$I_m=286$ A (main field is 800 G) due to the strong convergent field. This case corresponds to the highest density case mentioned earlier ($n_e=2.5\times10^{12}$ cm^{-3} with $P_{inp}=549$ W and $P_{Ar}=0.5$ mTorr). On the other hand, it will be possible to widen the plasma column further if the divergent field is applied near the antenna region. This will be a great advantage in that the diameters of a spiral antenna and a window can be much smaller than the diameter of the plasma column. We emphasize here that a helicon wave can propagate along the field lines in both convergent and divergent magnetic field configurations.[19]

The second method to control the radial electron density profile is to vary the radiation-field pattern of the antenna in two ways; one is to change the position and the number of turns of the spiral antenna used to radiate the rf fields, and the other is to switch the positions of the high voltage and ground feeding points. To test the effectiveness of the former technique, the results of the two experiments, in which the inner 2 spiral turns and the outer 2 spiral turns of the type *B* antenna are used, are compared in Fig. 3. The radial density profile in the case of the outer 2 turns is broader than that in the inner 2 turns. The radial profile, especially in the case of the outer 2 turns, often exhibits a hollow shape as can be seen in Fig. 3. Before (after) the density jump, the values of FWHM are 50 (41) cm and 45 (33) cm in the cases of the outer and the inner 2 turns, respectively. On the other hand, FWHM is found to be 41 cm in Fig. 3(b) without a hollow profile after the density jump when the full 4 spiral turns are used. This value lies between the cases of the inner 2 turns and the outer 2 turns in Fig. 3(b).

These different profiles reflect the variation of the antenna radiation-field pattern. E.g., in the case of the inner 2 turns, the region in which helicon waves are excited is expected to be narrower (constricted) in the radial direction.

Another way to change the radial density profile is to switch the positions of the high voltage and ground feeding points. We found that even when we used the same inner 2 spiral turns, the radial electron density profile showed a broader (and sometimes hollow) profile, as shown in Figs. 4(a) and 4(b), if the high-voltage side is connected to the outer position of the antenna and its center is grounded. This can be understood as being the result of the CCP generation effect, since a high voltage is applied to the outer 2 turns if the high voltage feeding position is the outer position of the 2 inner turns, even though there is no direct rf current in the outer 2 turns. However, as the rf power is increased, from Figs. 4(a) to 4(c), the CCP effect fades out due to the con-

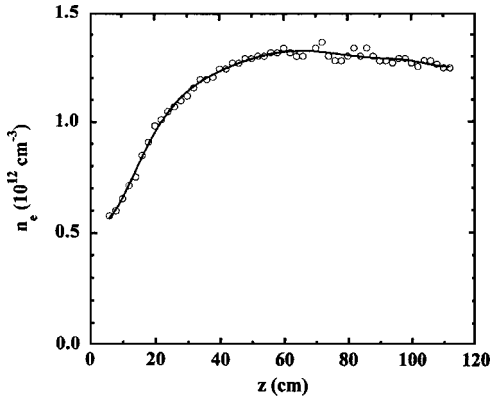

FIG. 5. Axial profile of n_e using the type *A* antenna with $P_{Ar}=2$ mTorr, $P_{inp}=390$ W, $I_m=50$ A, and $I_s=15$ A.

tribution of inductive and helicon generation effects becoming significant.

The features of the axial density profiles are described next. Figure 5 shows an example using the type *A* antenna. Along the *z* axis, n_e increases and reaches a maximum value of 1.35×10^{12} cm^{-3} at $z\sim60$ cm; then, it gradually decreases. Figure 6 shows the axial n_e profiles using the type *B* antenna before and after the density jumps. For the purely ICP case without a magnetic field (i.e., $I_m=I_s=0$ A) as shown in Fig. 6(a), the plasma decays monotonically along the *z* axis. Here, the *e*-folding length of the density decay is

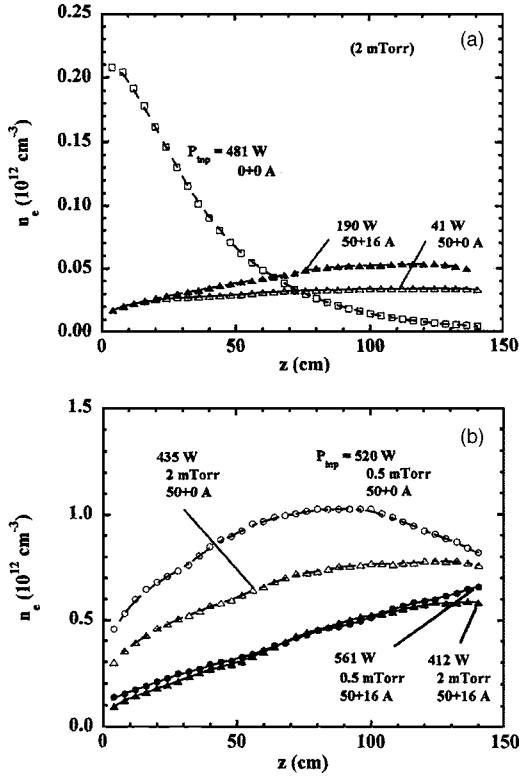

FIG. 6. Axial profiles of n_e using the type *B* antenna (a) before and (b) after the density jumps: (a) Open boxes, open triangles, and closed triangles show $(I_m,I_s)=(0\text{ A},0\text{ A})$, $(50\text{ A},0\text{ A})$, and $(50\text{ A},16\text{ A})$, respectively; (b) open and closed circles (open and closed triangles) denote $(I_m,I_s)=(50\text{ A},0\text{ A})$ and $(50\text{ A},16\text{ A})$, respectively, with $P_{Ar}=0.5(2)$ mTorr.

43 cm. On the other hand, with a background magnetic field, regardless of the magnetic field configuration and of the presence of density jumps or the discharge regimes, n_e increases along the *z* axis, and the axial position of the maximum n_e lies between 60 cm and 150 cm, depending on conditions, such as the fill pressure and the magnetic field geometry (degree of convergent field). Plasma uniformity along the *z* axis is very good: the decay length after the maximum density position is typically >100 cm. The decay length becomes even longer with a decrease in fill pressure, which is consistent with previous results,[11] and an increase in I_s (weaker convergent field). In order to achieve a uniform high-density plasma in the axial direction, it is better to have conditions (roughly) of $I_m>30$ A (main field is >84 G) and $I_s>10$ A, for the magnetic field.

To summarize, a high-density helicon plasma source with a very large volume, 75 cm in diameter and 486 cm in axial length, has been developed and the characteristics of this source have been investigated in detail. A plasma with an electron density of more than 10^{12} cm^{-3} has been successfully produced using several hundreds of watts of rf power. Control of the radial density profile has been carried out by varying the magnetic field configurations and the antenna field patterns.

This experiment was carried out at ISAS/JAXA under a research collaboration program. Encouragement from Professor Y. Nakamura, Professor Y. Kawai, Professor K. Oyama, and Professor K. Toki is greatly appreciated. The authors would also like to thank S. Sato, I. Funaki, and K. Aihara for their assistance in carrying out the experiments. The research was partially supported by the Grants-in-Aid for Scientific Research (B)(2) under the Contract Nos. 15340199 and 1435051 from the Japan Society for the Promotion of Science.

[1] R. W. Boswell, Appl. Phys. Lett. **33**, 457 (1970).
[2] R. W. Boswell, Plasma Phys. Controlled Fusion **26**, 1147 (1984).
[3] F. F. Chen, Plasma Phys. Controlled Fusion **33**, 339 (1991).
[4] A. Komori, T. Shoji, K. Miyamoto, and Y. Kawai, Phys. Fluids B **3**, 893 (1991).
[5] T. Shoji, Y. Sakawa, S. Nakazawa, K. Kadota, and T. Sato, Plasma Sources Sci. Technol. **2**, 5 (1993).
[6] M. A. Lieberman and A. J. Lichtenberg, *Principles of Plasma Discharges and Materials Processing* (Wiley, New York, 1994).
[7] S. Shinohara, Jpn. J. Appl. Phys., Part 1 **36**, 4695 (1997), and references therein.
[8] R. W. Boswell and F. F. Chen, IEEE Trans. Plasma Sci. **25**, 1229 (1997), and references therein.
[9] F. F. Chen and R. W. Boswell, IEEE Trans. Plasma Sci. **25**, 1245 (1997), and references therein.
[10] S. Shinohara, J. Plasma Fusion Res. **78**, 5 (2002), and references therein (mostly in Japanese).
[11] S. Shinohara, S. Takechi, and Y. Kawai, Jpn. J. Appl. Phys., Part 1 **35**, 4503 (1996).
[12] S. Shinohara, S. Takechi, N. Kaneda, and Y. Kawai, Plasma Phys. Controlled Fusion **39**, 1479 (1997).
[13] S. Shinohara and T. Tanikawa, Rev. Sci. Instrum. **75**, 1941 (2004).
[14] A. R. Ellingboe and R. W. Boswell, Phys. Plasmas **3**, 2797 (1996).
[15] J. Hopwood, Plasma Sources Sci. Technol. **1**, 109 (1992).
[16] S. Shinohara and K. Yonekura, Plasma Phys. Controlled Fusion **42**, 41 (2000).
[17] S. Shinohara and K. P. Shamrai, Plasma Phys. Controlled Fusion **42**, 865 (2000).
[18] K. P. Shamrai and S. Shinohara (private communication).
[19] S. Takechi and S. Shinohara, Jpn. J. Appl. Phys., Part 1 **38**, L1278 (1999).